PEG10 Activation by Co-Stimulation of CXCR5 and CCR7 Essentially Contributes to Resistance to Apoptosis in CD19^{+}CD34^{+} B Cells from Patients with B Cell Lineage Acute and Chronic Lymphocytic Leukemia

Chunsong Hu[1], Jei Xiong[2, 3], Linjei Zhang[1], Baojun Huang[1], Qiuping Zhang[3], Qun Li[1], Mingzhen Yang[4], Yaou Wu[1], Qun Wu[3], Qian Shen[1], Qingping Gao[5], Kejian Zhang[5], Zhimin Sun[6], Junyan Liu[3], Youxin Jin[2] and Jinquan Tan[1, 3, 7]

We investigated CD19^{+}CD34^{+} and CD19^{+}CD34^{-} B cells from cord blood (CB) and typical patients with B cell lineage acute and chronic lymphocytic leukemia (B-ALL and B-CLL) in terms of expression and functions of CXCR5/CXCL13 and CCR7/CCL19. CXCR5 and CCR7 were selectively frequent expressed on B-ALL, B-CLL and CB CD19^{+}CD34^{+} B cells, but not on CD19^{+}CD34^{-} B cells. Instead of induction of impressive chemotactic responsiveness, CXCL13 and CCL19 together induced significant resistance to TNF-α-mediated apoptosis in B-ALL and B-CLL but not CB CD19^{+}CD34^{+} B cells. B-ALL and B-CLL CD19^{+}CD34^{+} B cells expressed elevated level of Paternally Expressed Gene 10 (PEG10), and CXCL13 and CCL19 together significantly up-regulated PEG10 expression in the cells. We found that CXCL13 and CCL19 together by means of activation of CXCR5 and CCR7 up-regulated PEG10 expression and function, subsequent stabilized caspase-3 and caspase-8 in B-ALL and B-CLL CD19^{+}CD34^{+} B cells, and rescued the cells from TNF-α-mediated apoptosis. We suggested that normal lymphocytes, especially naïve B and T cells, utilized CXCR5/CXCL13 and CCR7/CCL19 for migration, homing, maturation, and cell homeostasis as well as secondary lymphoid tissues organogenesis. Meanwhile certain malignant cells took advantages of CXCR5/CXCL13 and CCR7/CCL19 for infiltration, resistance to apoptosis, and inappropriate proliferation. *Cellular & Molecular Immunology*. **2004;1(4): 280-294.**

Key Words: leukemia, B cells, chemokine receptor, apoptosis, chemotaxis

Introduction

CCL19 (Epstein-Barr virus-induced gene-1 ligand chemo kine, ELC) and CCL21 (secondary lymphoid tissue chemokine, SLC/6Ckine) are ligands for the chemokine receptor CCR7 (Burkitt lymphoma receptor-2, BLR2), whereas CXCL13 (B cell attracting chemokine 1, BCA-1) is probably the only ligand for CXCR5 (Burkitt's lymphoma receptor 1, BLR1) (1). Chemokines and their receptors are known as principal regulators of lymphocyte and dendritic cell (DC) migration in immune system homeostasis, infection, and inflammation (2). Homeostatic chemokines, such as CXCL13, CCL21, and CCL19, as well as their corresponding receptors, CXCR5 and CCR7, have been shown to closely cooperate in the development of lymphoid organs and the maintenance of lymphoid tissue microarchitecture (1). Expression of CXCR5 can be detected on mature re-circulating B cells, small subsets of

[1]Department of Immunology, College of Basic Medical Sciences, Anhui Medical University, Hefei 230032, China.

[2]The Stat Key Laboratory of Molecular Biology, Institute of Biochemistry and Cell Biology, Shanghai Institutes for Biological Sciences, Chinese Academy of Science, Shanghai, China.

[3]Department of Immunology, and Sino-Danish Joint Laboratory of Immunology, Wuhan University School of Medicine, Wuhan 430071, China.

[4]Department of Hematology, The Affiliated University Hospital, Anhui Medical University, Hefei 230031, China.

[5]Department of Hematology, The Renmin and Zongnan University Hospital, Wuhan University, Wuhan 430071, China.

[6]Department of Hematology, The Provincial Hospital of Anhui, Hefei 230020, China.

[7]Corresponding to: Dr. Jinquan Tan, Department of Immunology, and Sino-Danish Joint Laboratory of Immunology, Wuhan University School of Medicine, 430071 Wuhan or Department of Immunology, College of Basic Medical Sciences, Anhui Medical University, Meishan Road 69, Hefei 230032, China. Tel: +86-551-286-1139, Fax: +45-353-65326, E-mail: jinquan_tan@hotmail.com.

normal CD4^{+} and CD8^{+} T cells, and skin-derived migratory DCs (3-6). CXCL13 is expressed by follicular DCs (FDCs) and also other stromal cells located in the B-cell areas of secondary lymphoid organs (7, 8). CXCR5 is essentially responsible for guiding B cells into the B-cell zones of secondary lymphoid organs (9). However, the expression of CXCR5 on a subset of T cells strongly suggests a role for this receptor in T-cell migration as well (9, 10). CCR7 is highly expressed on naïve T cells and at lower levels on peripheral B cells. T cells and B cells show a transient increase in receptor expression following activation (11), whereas T-cell differentiation towards effector cells is accompanied by a downregulation of CCR7 on the cell surface (12). CCR7 expression is induced and increasingly upregulated upon maturation of DCs (13). The ligands for CCR7, CCL19 and CCL21, are constitutively expressed by stromal cells within the T-cell zones of secondary lymphoid organs. CCL19 is expressed by DCs in the T-cell zones, whereas CCL21 can be secreted by endothelial cells of high endothelial venues (HEVs) and lymphatic vessels (14). CCR7 not only mediates T-cell and DC homing to the T-cell zones of secondary lymphoid organs but also mediates B-cell entry into the spleen and peripheral lymph nodes (1). CXCR5 cooperating with CCR7 controls lymphocyte and DC homing to secondary lymphoid organs including lymph nodes and Peyer's patches, and functions lymphoid organ organogenesis and organization (11, 15). CXCL13/BCA-1, which is responsible for compartmental homing of CXCR5-bearing B lymphocytes and directing T-helper cells into the lymphoid follicle (7-10, 16, 17), is also found to highly express on malignant lymphocytes and vascular endothelium in primary central nervous system lymphoma (18). High-level expression of CXCR5-CXCL13/BCA-1 pair is observed in all mucosal lymphoid aggregates and in the mantle zone of all secondary lymphoid follicles in Hp-induced gastric mucosa-associated lymphoid tissue (19). CCR7 is found to be over-expressed, involving in lymphoid organ infiltration of adult T-cell leukemia cells (20). CCR7 and α4 integrin are important for migration of CLL cells into lymph nodes (21). However, the functional importance of CXCR5-CXCL13/BCA-1 and CCR7-CCL19/ELC receptor-ligand pairs in the pathophysiological events of malignant T cell trafficking, homing, and survival is not fully understood.

A novel paternally expressed imprinted gene, Paternally Expressed Gene 10 (PEG10), is identified as a paternally expressed gene from a newly defined imprinted region at human chromosome 7q21 (22). PEG10 is located near the SGCE (Sarcoglycan e) gene, whose mouse homologue is also recently shown to be imprinted (22). PEG10 shows parent-of-origin-specific expression in monochromosomal hybrids (23). It has been found an elevated level of expression in the majority of the human hepatocellular carcinoma cells (HCC) (24, 25), and G2/M phase of regenerating mouse liver (25). Exogenous expression of PEG10 confers oncogenic activity and transfection of hepatoma cells with PEG10 antisense suppressing its expression results in cancer cell growth inhibition (24). PEG10 protein associates with SIAH1, a mediator of apoptosis. Overexpression of PEG10 decreases the cell death mediated by SIAH1 (24).

Materials and Methods

Patients and cell purification

All patients with B-ALL fulfilled The French-American-British (FAB) Cooperative Group criteria (26). Age range of patients was 22 to 65 years with 14 males and 9 females. All patients with B-CLL were diagnosed according to the guidelines of the National Cancer Institute Working Group on B-CLL and classified according to the FAB classification proposed in 1989 (27, 28). Age range of patients was 18 to 62 years including 12 males and 6 females. All patients were informed consent according to institutional guidelines. CD19^{+} or CD19^{+}CD34^{+} cells were purified PBMCs as described elsewhere (29, 30). The PBMCs were from peripheral blood of normal subjects, cord blood (CB) of uncomplicated births (IgM undetectable) or patients with B-ALL or B-CLL. After enrichment of PBMCs by LymphPrep™ gradient, CD19^{+} or CD19^{+}CD34^{+} double-positive cells were sorted using a FACSstarPlus and FITC- or PE-conjugated antibodies (BD Pharmingen) against CD19 and CD34. The viability of all cultured cells > 95% tested by trypan blue exclusion. The purity of the cells ranged from 90% to 99%, as determined by flow cytometry. The malignancy of purified B-ALL or B-CLL CD19^{+}CD34^{+} cells was checked by expression of CD25, CD45RO and HLA-DR (29). The cell line was malignant mammary cell line ER-alpha^{+} MCF7-Fas cells obtained from the American Type Culture Collection (Manassas, VA, USA). The a-CXCR5 and a-CCR7 mAbs and chemokines (CXCL13/BCA-1, CCL19/ELC, CCL25/TECK and CXCL12/SDF-1) were purchased from R&D Systems, Abingdon, UK.

Flow cytometry

For detection of CXCR5 and CCR7, the cells were triple stained PE-labeled CD19, FITC-labeled CD34 (DAKO, Denmark) and PerCP-labeled chemokine receptor antibody (R&D Systems, Abingdon, UK), or matched isotype antibody (DAKO) at 5 μg/ml in PBS containing 2% BSA and 0.1% sodium azide for 20 min, followed washing twice in staining buffer (30). The analyses were performed with a flow cytometer (COULTER® XL, Coulter Corporation, Miami, FL, USA). For detection of apoptosis, cells were stained in staining medium (RPMI 1640, 2% FBS and 0.1% sodium azide) with 1 μg/ml propidium iodide (PI) for 30 min at 4°C, then stained with FITC-conjugated annexin V with binding buffer (BD Pharmingen) as previously described (31, 32). COULTER® XL was used for analyses. For detection of intracellular active caspases, cytofix/cytoperm buffer (BD Pharmingen) was used according to the manufacturer's instructions to permeabilize cells, and cells were subsequently stained with anti-active-capsase-3 or anti-active-caspase-8 monoclonal antibody (BD Pharmingen). After washing, active caspase-3 or caspase-8 fluorescence intensity was measured by flow cytometry. Data were analyzed by means of the WinList program (The Scripps Research Institute, La Jolla, CA, USA).

Real time quantitative RT-PCR assay

All real time quantitative RT-PCR reactions were performed as described elsewhere (30, 33). Briefly, total RNA from

purified cells (1×10^5, purity > 99%) was prepared by using Quick Prep® total RNA extraction kit (Pharmacia Biotech, USA) according to the manufacturer's instructions. RNA was reverse transcribed by using oligo (dT) 12-18 and Superscript II reverse transcriptase (Life Technologies, Grand Island, USA). The real time quantitative PCR was performed in special optical tubes in a 96 well microtiter plate (Applied Biosystems, Foster City, CA, USA) with an ABI PRISM® 7700 Sequence Detector Systems (Applied Biosystems). By using SYBR® Green PCR Core Reagents Kit, fluorescence signals were generated during each PCR cycle via the 5´ to 3´ endonuclease activity of AmpliTaq Gold to provide real time quantitative PCR information. The sequences of the specific primers listed below. CXCR5 sense: 5'-GGT CTT CAT CTT GCC CTT TG-3'; antisense: 5'-ATG CGT TTC TGC TTG GTT CT-3'. CCR7 sense: 5'-GCT CCA GGC ACG CAA CTT T-3'; antisense: 5'-ACC ACG ACC ACA GCG ATG A-3'. PEG10 sense: 5'-ATG ATG ACA TCG AGC TCC G-3'; antisense: 5'-GCT GGG TAG TTG TGC ATC A-3'.

All unknown cDNAs were diluted to contain equal amounts of β-actin cDNA. The standards, "no template" controls and unknown samples were added in a total volume of 50 µl per reaction. PCR retain conditions were 2 min at 50°C, 10 min at 95°C, 40 cycles with 15 s at 95°C, 60 s at 60°C for amplifications. Potential PCR product contamination was digested by uracil-N-glycosylase (UNG) since dTTP is substituted by dUTP. UNG and AmpliTaq Gold (Applied Biosystems) were applied according to the manufacturer's instructions.

Northern and Western blot assays
For mRNA detection (Northern blot), as previously described (29, 34), each 5 µg of total RNA were electrophoresed under denaturing conditions, followed by blotting onto Nytran membranes, and cross-linked by UV irradiation (34). CXCR5 and CCR7 cDNA probes, labeled by α-(^{32}P)dCTP, were obtained by PCR amplification of the sequence mentioned above from total RNA from PBMC from normal adults (for CXCR5) or thymocytes from the specimen of thymusectomy (for CCR7), or human heaptoma cell line HepG2 (for PEG10). The membranes were hybridized overnight with 1×10^6 cpm/ml of ^{32}P-labeled probe, followed by intensively washing with $0.2 \times$ SSC and 0.1% SDS before being autoradiographed. For protein detection (Western blot) the cells were lysed in lysis buffer. Cell lysis was performed for 30 min at 4°C with lysis buffer (25 mM HEPES (pH 7.6), 1% Triton X-100, 137 mM NaCl, 3 mM β-glycerophosphate, 3 mM ethylenediaminetetraacetic acid, 0.1 mM sodium orthovanadate, 1 mM phenylmethylsulfonyl fluoride). Expression of IAP family proteins (or other proteins indicated) was semi-quantified after Western blot analysis (35). Lysates were centrifuged at 10,000 rpm for 5 min at 4°C. Protein concentration was measured by Bio-Rad protein assay. Protein (around 40 µg) was loaded onto 16% SDS-PAGE, transferred onto PVDF membranes after electrophoresis, and incubated with the appropriate Abs at 0.5 µg/ml. Analyses were conducted using enhanced chemiluminescence detection (Amersham Pharmacia Biotech, Little Chalfont, UK). All Abs (Bcl-2, Bcl-X, c-FLIP$_L$, c-IAP1, c-IAP2, XIAP, and

survivin) were from Santa Cruz Biotech. Inc. Santa Cruz, CA, USA, except a-livin was from Imgenex Corp. Sorrento Valley, San Diego, USA, and a-β-actin was from Sigma Chemical Co., and CXCR5 and CCR7 mAbs were from R&D Systems.

Immunofluoescence digital confocal microscopy
As described elsewhere (29, 36), the purified cells were spun down on a slide, fixed with a mixture of methanol and acetone, immersed in 1% BSA blocking buffer for 10 min to avoid non-specific binding, added antibody either FITC-labeled CXCR5, CCR7 mAb or isotype IgG2a at 10 µg/ml, and incubated overnight at 4°C. The preparations were observed using a fluorescence microscope (model BX60, Olympus, Japan). Confocal microscopy analysis was performed using a confocal laser scanning system and an inverted microscope (model LSMSIO, Zeiss, Germany). Images of serial cellular section were acquired with the Bio-Rad Comos graphical user-interface as described (29, 36).

Chemotaxis assay
The chemotaxis assay was performed in a 48-well micro-chamber (Neuro Probe, Bethesda, MD) technique (29, 31). Briefly, chemokines in RPMI 1640 with 0.5% BSA was placed in the lower wells (25 µl). 25 ml cell suspension (2×10^6 cells/ml) was added to the upper well of the chamber, which was separated from the lower well by a 5 µm pore-size, polycarbonate, polyvinylpyrolidone-free membrane (Nucleopore, Pleasanton, CA, USA). The chamber was incubated for 60 min at 37° C and 5% CO_2. The membrane was then carefully removed, fixed in 70% methanol and stained for 5 min in 1% Coomassie brilliant blue. The migrating cells were counted using a light microscopy. Approximately 6% of the cells will migrate spontaneously (known as MCNC). The results were expressed as C.I. with standard deviation (SD).

PNA antisense assay
As previously described with a modification (37), cells were permeabilized with a buffered solution containing a relatively low concentration of detergent (0.05% Tween 20), then cultured in RPMI 1640 with 10% FCS in the presence of antisense PNA (Applied Biosystems) at different concentrations (0.02 µM or 2 µM) with or without stimuli for 6 days. PNAPEG10 antisense sequences used was as follow: 5´-$_{NH2}$-TCTGCACCTGGCTCTG-$_{COOH}$-3´. DNA livin antisense sequence (DNAPEG10) used was identical to PNAPEG10 (concentration 2 µM). PNA mismatch sequence: 5´-$_{NH2}$-ACTTCTCAGTCTGCTT-$_{COOH}$-3´ (randomly synthesized, concentration 2 µM). Cells were extensively washed prior to the procedures prior to further assays. The viability of the cells was > 95% checked by a trypan blue exclusion test.

Plasmids and cell transfection
Plasmids encoding PEG10, CXCR5, and CCR7 used in this study have been previously described (25, 38, 39). The cells were transiently transfected with vectors encoding target genes as described elsewhere (25, 38, 39). Briefly, the cells were cultured with DMEM containing 10% FCS,
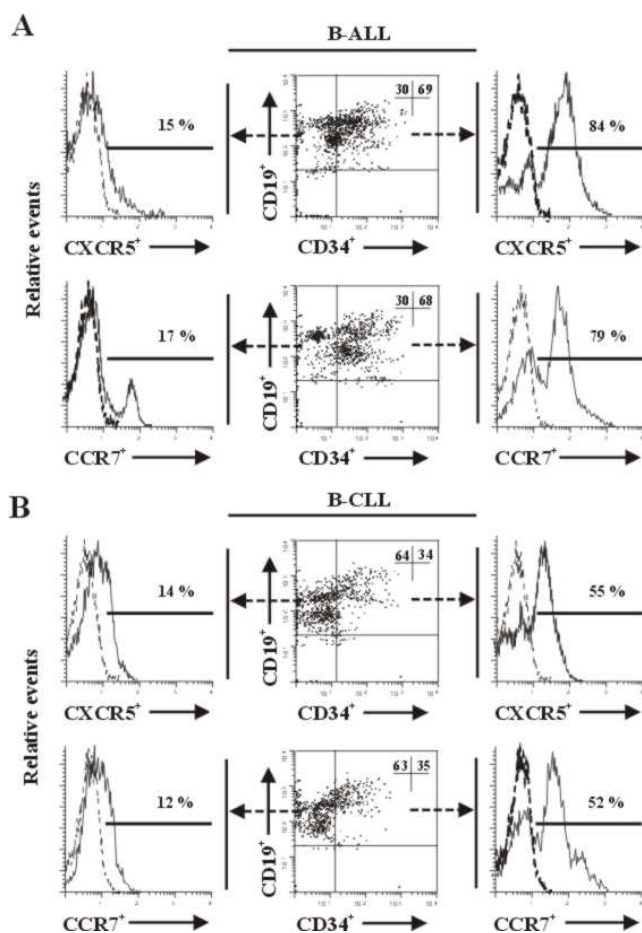
Figure 1. CXCR5 and CCR7 distribution on CD19⁺CD34⁺ and CD19⁺CD34⁻ B cells. Triple-color flow cytometric analysis of the distribution of CXCR5 and CCR7 on CD19⁺CD34⁺ and CD19⁺CD34⁻ B cells from B-ALL (A) and B-CLL (B) patients. The CD19⁺ B cells were freshly isolated and stained in triple colors of CD19 (PE), CD34 (FITC) and CXCR5 or CCR7 (PerCP) as described in *Materials and Methods*. The indicated numbers in the graphs were percentages of CD19⁺CD34⁺ and CD19⁺CD34⁻ B cells. The indicated percentages in the graphs were numbers of CXCR5⁺ or CCR7⁺ B cells. The data were from a single experiment, which was representative of 23 (B-ALL) and 18 (B-CLL) similar experiments performed. Isotype Ab controls were expressed as dished curves.

Table 1. *Some chemokine receptor expression on $CD19^+CD34^+$, $CD19^+CD34^-$ B cells*[a].

Cell type[b]	CXCR3	CXCR5	CXCR6	CCR4	CCR7	CCR9
Periphery						
CD19⁺CD34⁺	N.D.[c]	N.D.	N.D.	N.D.	N.D.	N.D.
CD19⁺CD34⁻	4 ± 1[d]	7 ± 2	13 ± 8	10 ± 1	6 ± 4	-[e]
CB						
CD19⁺CD34⁺	22 ± 10	51 ± 14	28 ± 17	10 ± 2	60 ± 15	24 ± 12
CD19⁺CD34⁻	10 ± 10	20 ± 11	15 ± 5	-	22 ± 12	-
B-ALL						
CD19⁺CD34⁺	75 ± 21	85 ± 12	85 ± 12	79 ± 15	79 ± 15	-
CD19⁺CD34⁻	34 ± 18	31 ± 16	14 ± 7	21 ± 12	28 ± 13	-
B-CLL						
CD19⁺CD34⁺	61 ± 17	51 ± 15	27 ± 13	25 ± 14	45 ± 18	2 ± 1
CD19⁺CD34⁻	7 ± 6	11 ± 5	5 ± 2	11 ± 8	12 ± 10	4 ± 2

a. The CD19⁺CD34⁺, CD19⁺CD34⁻ B cells were freshly isolated and stained in triple colors of CD19 (PE), CD34 (FITC) and indicated chemokine receptor antibodies (PerCP) as described in *Materials and Methods*.
b. the CD19⁺ B cells were isolated from peripheral blood from normal subjects, cord blood (CB) of uncomplicated births, B-ALL or B-CLL patients.
c. N.D., no determination since few CD19⁺CD34⁺ B cells in normal preipheral blood.
d. the listed numbers in the table were percentages of chemokine receptor positive B cells. The data were mean values ± SD at least of eight similar experiments conducted. For detection of CXCR5 or CCR7, showing data were mean values ± SD of 20 B-ALL and 15 B-CLL patients.
e. under detectable level.

penicillin, and streptomycin. Cells were grown to approximately 70% confluence in 60-mm dishes for 24 hours before transfection. The DNA constructs of expression vectors (0.4 µg unless indicated) or vector only was mixed with 12 µl of LipofectAMINE (Gibco BRL) in 2 ml of opti-DMEM serum-free medium and added to cells, and incubated for 6 hours. The cells were further cultured in 2.5 ml of DMEM containing 10% FCS in 5% CO_2.

Results

CXCR5 and CCR7 were selectively frequent expressed on B-ALL and B-CLL CD19⁺CD34⁺ B cells
We examined the expression of CXCR5 and CCR7 on purified CD19⁺CD34⁺, and CD19⁺CD34⁻ B cells from

B-ALL or B-CLL patients. In total 41 cases of typical B-ALL and B-CLL patients, flow cytometric analysis (Figure 1 and Table 1) revealed that the percentages of CD19⁺CD34⁺ B cells from patients with B-ALL were higher than that from patients with B-CLL. Interestingly, CXCR5 and CCR7 were selectively frequent expressed on B-ALL and on B-CLL CD19⁺CD34⁺ B cells (84%, 79%, 55% and 52%, respectively) (Figure 1A and 1B), whereas, B-ALL and B-CLL CD19⁺CD34⁻ B cells expressed significantly lower frequent CXCR5 and CCR7 (15% and 17%, 14% and 12%, respectively). We also examined the expression of CXCR5 and CCR7 on CD19⁺CD34⁺ and CD19⁺CD34⁻ B cells from CB of uncomplicated births as well as CD19⁺ B cells from normal peripheral blood. As what shown in Table 1, CXCR5 and CCR7 were at rather low level on CD19⁺ B cells from normal peripheral blood, whereas they were expressed a similar levels on the on CD19⁺CD34⁺ and CD19⁺CD34⁻ B cells from CB. We also screened other CXC and CC chemokine receptors. As what shown in Table 1, the data for CXCR3, CXCR6, CCR4 and CCR9 were either in agreements with previous reports or no differences among four types of cell sources.

To be sure the obtained results, we first conducted the real time quantitative RT-PCR assay to detect the different expressions of CXCR5 and CCR7 at mRNA levels. CXCR5 and CCR7 mRNA were detected at very low levels in freshly isolated normal peripheral CD19⁺ B cells. CXCR5 and CCR7 mRNA in CD19⁺CD34⁺ B cells from normal blood CB, B-ALL and B-CLL were significantly upregulated (Figure 2A), whereas, they in CD19⁺CD34⁻ B cells had no significant difference from that in normal peripheral B cells
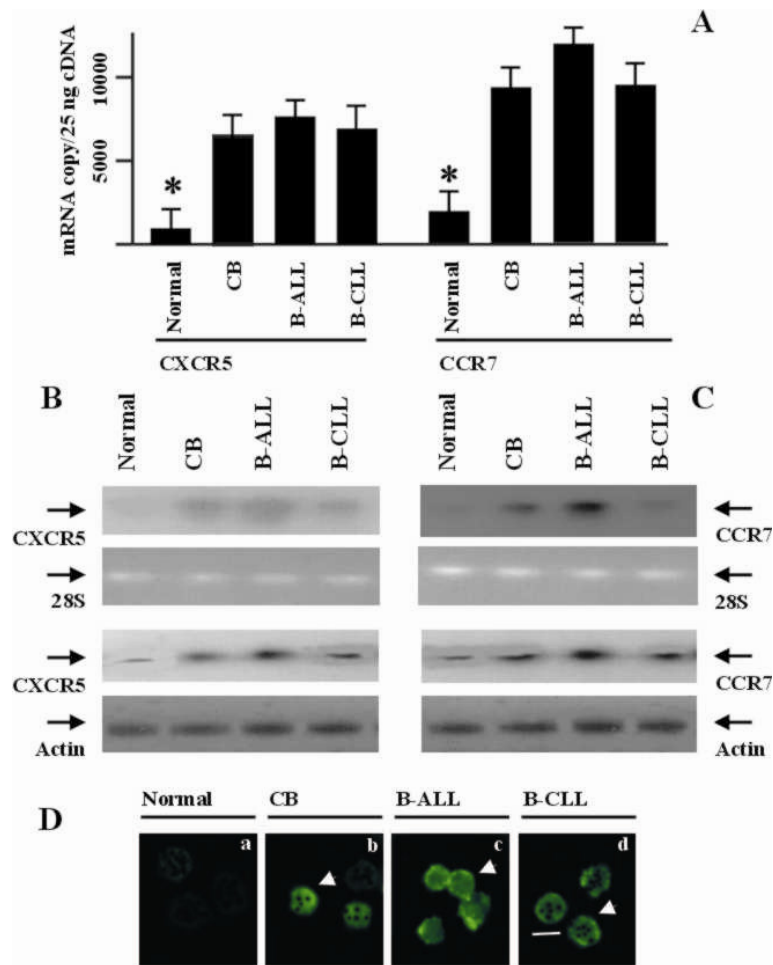
Figure 2. CXCR5 and CCR7 expression on CD19⁺CD34⁺ B cells. CXCR5 and CCR7 expression on CD19⁺CD34⁺ B cells were examined by real time quantitative RT-PCR (A), Northern blot (B, C; upper panels), Western blot (B, C; lower panels), and confocal microscopy (D). The CD19⁺CD34⁺ T cells were freshly isolated from normal PBMC (only CD19⁺), cord blood (CB) of uncomplicated births, B-ALL or B-CLL patients as described in *Materials and Methods*. In A, the procedure for quantitative RT-PCR amplification was described in *Materials and Methods*. A linear relationship between C_T and log starting quantity of standard DNA template or target cDNA (CXCR5 or CCR7) was detected (data not shown). The showing bars were mean values ± SD of eight similar experiments conducted. In B and C (upper panels), the detections of mRNA of CXCR5 and CCR7 were by Northern blot for freshly isolated CD19⁺CD34⁺ B cells from normal PBMC (only CD19⁺), cord blood (CB) of uncomplicated births, B-ALL or B-CLL patients. Total RNA from different cells were isolated, electrophoresed and blotted as described in *Materials and Methods*. The hybridization signals for CXCR5 or CCR7 mRNA from different cells were shown in upper pictures. The 28S rRNAs in lower pictures confirmed that comparable amounts of total RNA were used. In B and C (lower panels), The CXCR5 or CCR7 protein was examined using Western blot analyses. The cells, from different subjects as described above, were lysed and total protein content electrophoresed and blotted as described in *Materials and Methods*. Actins in lower pictures indicated the quantity of total cellular protein from the tested samples loaded in each lane. Arrows indicated markers used to verify equivalent molecular weights of appropriate proteins in each lane. In D (upper parts), for confocal microscopy the CD19⁺CD34⁺ B cells were purified from different subjects as indicated (only CD19⁺ from normal PBMC), and stained as described in *Materials and Methods*. The cells were photographed under epi-fluorescent conditions. Original magnification: × 1,200. Bar, 11 μm. The arrows are indicating typical CXCR5⁺ positive cells. The lower parts in imagines were isotype Ab controls. The imagines were taken in a single experiment, which was a representative of experiments on each 6 of normal PBMC, CB blood, B-ALL and B-CLL patients.

(data not shown). The same patterns of CXCR5 and CCR7 mRNA expression in distinct cells were seen in Northern blot (Figure 2B and 2C, upper panels). An elevated CXCR5 and CCR7 protein expression in B-ALL and B-CLL CD19⁺CD34⁺ B cells were also observed in Western blot (Figure 2B and 2C, lower panels). The CXCR5 and CCR7 expression pattern in CD19⁺CD34⁻ B cells from distinct subjects (see Figure 1 and Table 1) were also confirmed by Northern and Western blots (data not shown). CXCR5 was rarely expressed on normal peripheral CD19⁺ B cells detected

by immunofluroescence digital confocal microscopy (Figure 2Da). In contrast, CXCR5 was frequently expressed on CD19⁺CD34⁺ B cells from normal CB (Figure 2Db), B-ALL patient (Figure 2Dc), and B-ALL patient (Figure 2Dd). All CD19⁺CD34⁺ B cells in a representative field were showing CXCR5 positive (Figure 2Dc and 2Dd), whereas 2 of 3 CB CD19⁺CD34⁺ T cells in a representative field were showing CXCR5 positive (Figure 2Db). We also observed same pattern of CCR7 expression on CD19⁺CD34⁺ B cells from distinct cell sources (data not shown). Thus, CXCR5 and
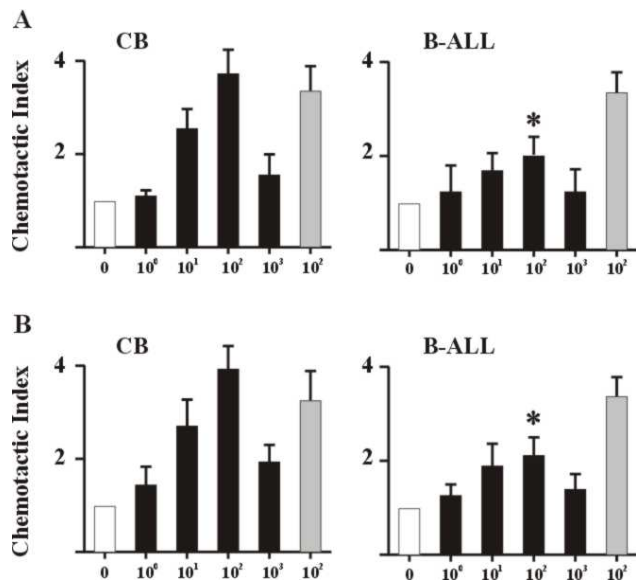
Figure 3. The chemotaxis of CD19+CD34+ B cells. The chemotaxis of freshly isolated in CD19+CD34+ T cells from cord blood (CB) of uncomplicated births and B-ALL patients towards CXCL13/BCA-1 (A) (solid bars), CCL19/ELC (B) (solid bars), CCL3/MIP-1α (gray bars) (100 ng/ml) or PBS control (open bars). All results were determined as described in *Materials and Methods* and expressed as Chemotactic Index (C.I.) or percentage of adhesive cells with Standard Deviation (± SD), and based on triplicate determination of chemotaxis and adhesion on each concentration of chemokine indicated as ng/ml. The results were sums of eight experiments conducted. Statistical significant differences as compared to controls are indicated * $p < 0.001$. Values $p > 0.05$ are considered non-significant.

CCR7 were selectively frequent expressed on B-ALL and B-CLL CD19+CD34+ B cells.

CXCL13/BCA-1 and CCL19/ELC induced weak chemotaxis in B-ALL and B-CLL CD19+CD34+ B cells

Most chemokines had been demonstrated to induce chemotaxis of inflammatory cells by upregulating chemokine receptor expression (2). We also observed that CCL25/TECK induced selectively T-ALL CD4+ T cell chemotaxis, where CCR9 was highly expressed (29). To investigate the biological effects of CXCR5 and CCR7 on B-ALL and B-CLL CD19+CD34+ B cells, we studied the functional activities of CXCR5 and CCR7 on these cells. The CXCR5 ligand, CXCL13/BCA-1, induced a very weak chemotaxis in freshly isolated B-ALL CD19+CD34+ B cells, whereas CCL3/MIP-1α, a ligand for CCR5 which was reported to be highly expressed on B-ALL CD19+ B cell, had a significant chemotactic effect on B-ALL CD19+CD34+ B cell (Figure 3A, right panel). Interestingly, CXCL13/BCA-1 induced a very strong chemotaxis in freshly isolated CB CD19+CD34+ B cells, as well as CCL3/MIP-1α had a significant chemotactic effect on the cells (Figure 3A, left panel). Moreover, the CCR7 ligand CCL19/ELC, induced only a very weak chemotaxis in freshly isolated B-ALL CD19+CD34+ B cells (Figure 3B, right panel). Interestingly, CCL19/ELC induced a very strong chemotaxis in freshly isolated CB CD19+CD34+ B cells (Figure 3B, left panel).
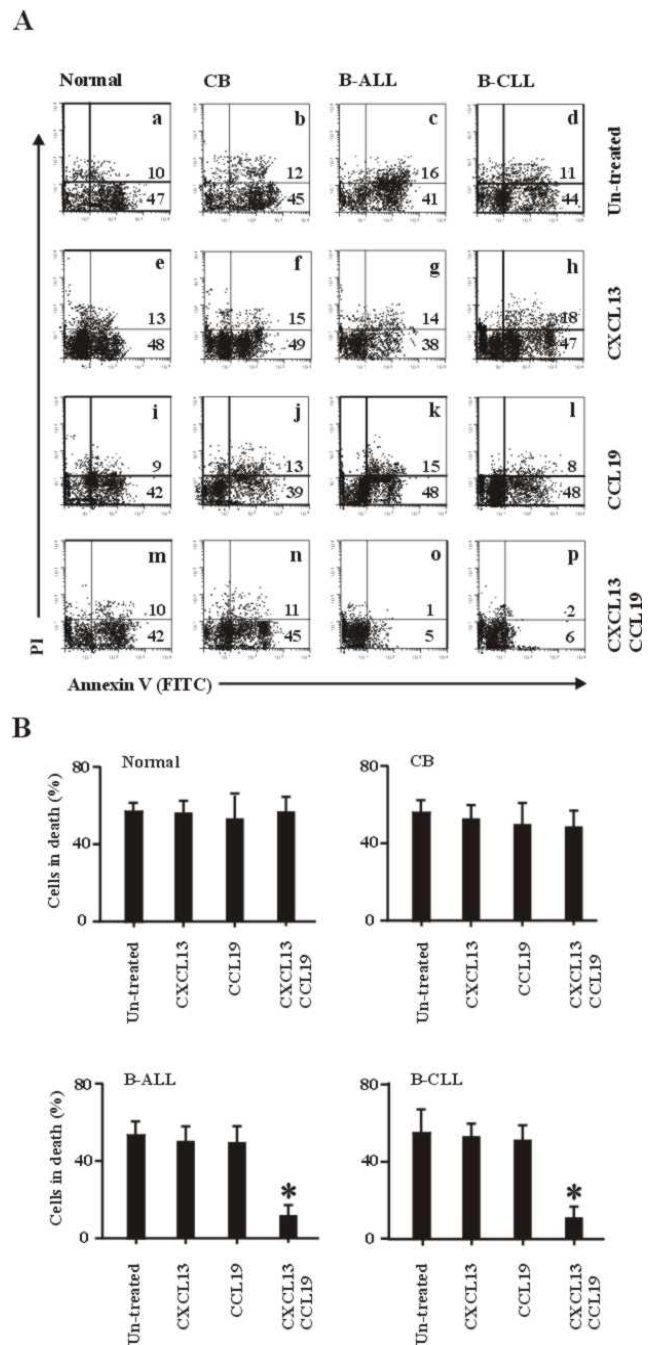

Figure 4. Analysis of apoptotic and total dead (necrotic and apoptotic) cells in CD19+CD34+ B cells. Flow cytometric analysis of apoptotic (A) and total dead cells (B), the CD19+CD34+ B cells were freshly isolated from normal PBMC (only CD19+), cord blood (CB) of uncomplicated births, B-ALL or B-CLL patients as described in *Materials and Methods*, which were pre-treated at absence or presence of chemokine as indicated (all at 100 ng/ml) for 24 h at 37° C, following stimulation with TNF-α (100 ng/ml) for 24 h at 37° C. The cells were analyzed by flow cytometry for PI (*y* axis) and FITC-conjugated annexin V (*x* axis) as described in *Materials and Methods*. The gating in the forward scatter and side scatter histograms were adhered to the lymphocyte region. The percentages of PI- annexin V+ cells and PI+ annexin V+ cells were indicated in the figure. The data (A) were from a single experiment, which was representative of six experiments performed. The data for total dead cells (PI- annexin V+ + PI+ annexin V+) (B) were mean values ± SD of six experiments performed. Statistically significant differences as compared with un-treated cells were indicated (* $p < 0.001$).

CXCL13/BCA-1 and CCL19/ELC together also failed to induce strong chemotaxis in freshly isolated B-ALL and B-CLL CD19^{+}CD34^{+} B cells (data not shown). Thus, CXCR5-CXCL13/BCA-1 pair and CCR7-CCL19/ELC pairs had no "common" strong chemotactic functions in B-ALL and B-CLL CD19^{+}CD34^{+} B cells.

CXCL13/BCA-1 and CCL19/ELC together selectively rescued B-ALL and B-CLL CD19^{+}CD34^{+} B cells from TNF-α-mediated apoptosis

By knowing that some of chemokine receptors such as activation of CCR9 led to phosphorylation of GSK-3β and FKHR and provided a cell survival signal (31), and that selective frequently CXCR5 and CCR7 expressed on B-ALL and B-CLL CD19^{+}CD34^{+} B cells, which had no significant "common" chemotactic functions in the cells, we examined the protective effects of CXCL13/BCA-1, CCL19/ELC, CCL3/MIP-1α, and CXCL12/SDF-1 (31) on different types of cells on TNF-α-mediated apoptosis. Flow cytometric analysis (Figure 4) revealed that the number of apoptotic and necrotic cells were significantly decreased in culture of B-ALL and B-CLL CD19^{+}CD34^{+} B cells in the presence of CXCL13/BCA-1 and CCL19/ELC together (Figure 4 Ao and Ap), in comparison with that in the absence of CXCL13/BCA-1 and CCL19/ELC (Figure 4 Ac and Ad). Interestingly, CXCL13/BCA-1 or CCL19/ELC alone had no such function in B-ALL and B-CLL CD19^{+}CD34^{+} B cells (Figure 4 Ag, Ah, Ak and Al). CXCL13/BCA-1 or/and CCL19/ELC induced no resistance to TNF-α-mediated apoptosis in normal peripheral CD19^{+} B cells and CB CD19^{+}CD34^{+} B cells (Figure 4 Ae, Af, Ai, Aj, Am, and An), in comparison with that in the absence of CXCL13/BCA-1 and CCL19/ELC together (Figure 4 Aa and Ab). Neither CCL3/MIP-1α nor CXCL12/SDF-1 had such function to rescue different type of B cells (normal peripheral CD19^{+} B cells, and CB, B-ALL B-CLL CD19^{+}CD34^{+} B cells) from TNF-α-mediated apoptotic response (data not shown). Abs against CXCR5 and CCR7 could completely block the protective effect of CXCL13/BCA-1 and CCL19/ELC together, indicating that rescuing effect was indeed induced by means of interaction of CXCL13/CCL19 and CXCR5/CCR7 (data shown in Figure 5). As shown in Fig. 4B, the total fractions of dead cells (including apoptotic and necrotic) in different types of the cells tested were the same patterns as the results in Figure 4A. These results could show again that CXCL13/BCA-1 and CCL19/ELC together selectively rescued B-ALL and B-CLL CD19^{+}CD34^{+} B cells from TNF-α-mediated apoptosis, but not either normal peripheral CD19^{+} B cells or CB CD19^{+}CD34^{+} B cells, confirming the count-effects of CXCR5 and CCR7 together on death signaling of TNF-α in B-ALL and B-CLL CD19^{+}CD34^{+} B cells.

Many signaling events of binding of certain chemokines to chemokine receptors were included such as PI-3 kinase, MAPK, or PKC, that appearing to be involved in chemokine-mediated chemotaxis in certain cell types (40-43). We intended to use some specific signaling pathway inhibitors to elucidate through which involvement of activated downstream substrates in the protective effects from apoptosis. To determine whether these kinases were responsible for resistance to apoptosis induced by
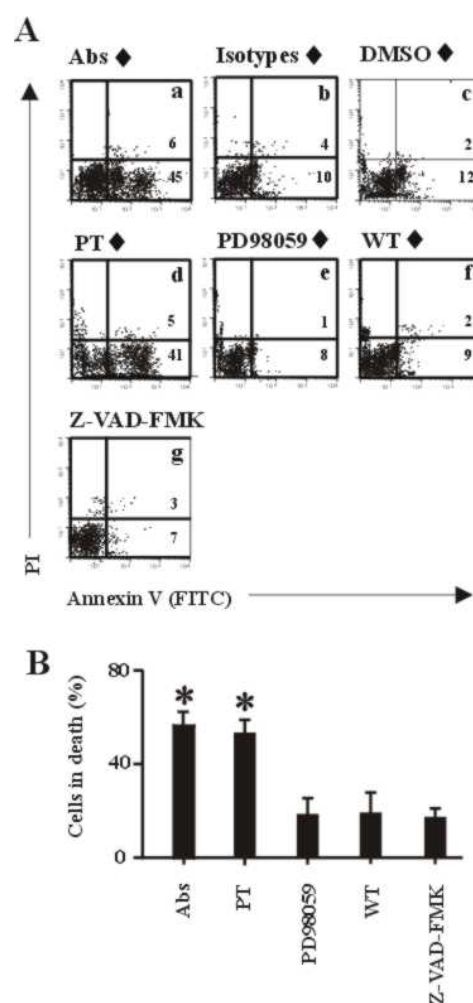

Figure 5. Analysis of apoptotic and total dead (necrotic and apoptotic) cells for inhibition of TNF-α-mediated apoptosis of CD19^{+}CD34^{+} B cells. Flow cytometric analysis of apoptotic (A) and total dead cells (B), B-ALL CD19^{+}CD34^{+} B cells were freshly isolated from B-ALL patients as described in *Materials and Methods*, then serum starved overnight and treated with a-CXCR5 plus a-CCR7 (each 5 μg/ml, Abs), isotype Abs (each 5 μg/ml, Isotypes), pertussis toxin (PT) (1 μg/ml), wortmannin (WT, 50 nM), PD98059 (50 μM), or vehicle DMSO for 1 hour, followed culture in the presence of CXCL13/BCA-1 and CCL19/ELC (♦, each 100 ng/ml) for 6 hours before apoptotic assay. As a control, Z-VAD-FMK (20 μM), a caspase inhibitor, was used for blocking apoptosis. The cells were analyzed by flow cytometry for PI (*y* axis) and FITC-conjugated annexin V (*x* axis) as described in *Materials and Methods*. The percentages of PI[-] annexin V^{+} cells and PI[+] annexin V^{+} cells were indicated in the figure. The data were from a single experiment, which was representative of six experiments performed. The data for total dead cells (PI[-] annexin V[+] + PI[+] annexin V[+]) (B) were mean values ± SD of six experiments performed. Statistically significant differences as compared with un-treated cells were indicated (∗ *p* < 0.001).

co-stimulation of CXCL13/BCA-1 and CCL19/ELC, B-ALL and B-CLL CD19^{+}CD34^{+} B cells were pre-treated with varying concentrations of pertussis toxin, an inhibitor of PKC; wortmannin, a potent PI-3 kinase inhibitor; PD98059, a MAPK inhibitor; or vehicle, DMSO before cell co-stimulation with CXCL13/BCA-1 and CCL19/ELC. As

seen in Figure 5A, only pertussis toxin significantly inhibited apoptotic protection effect of co-stimulation with CXCL13/BCA-1 and CCL19/ELC in B-ALL CD19+CD34+ B cells. Neither PD98059 nor wortmannin did inhibit apoptotic protection effect in B-ALL CD19+CD34+ B cells, suggesting that CXCL13/BCA-1 and CCL19/ELC together went through PKC signaling pathways to carry out apoptotic protection in B-ALL CD19+CD34+ B cells. As expected, Z-VAD-FMK rescued B-ALL CD19+CD34+ B cells from TNF-α-mediated apoptosis. We observed similar results in B-CLL CD19+CD34+ B cells (data not shown). As expected, mAbs against CXCR5 and CCR7 together significantly inhibited apoptotic protection effect of co-stimulation with CXCL13/BCA-1 and CCL19/ELC in B-ALL CD19+CD34+ B cells, whereas isotypes had no such effect (Figure 5Aa and Ab), documenting that apoptotic protection effect of CXCL13/BCA-1 and CCL19/ELC in the cells was indeed by means of CXCR5 and CCR7. As shown in Figure 5B, the data of total fractions of dead cells (including apoptotic and necrotic) were the same pattern as the results in Figure 5A. These results could show again that CXCL13/BCA-1 and CCL19/ELC together interacted with CXCR5 and CCR7 to rescue B-ALL and B-CLL CD19+CD34+ B cells from TNF-α-mediated apoptosis by means of PKC signaling pathways.

PEG10 expression in B-ALL and B-CLL CD19+CD34+ B cells was selectively increased by CXCL13/BCA-1 and CCL19/ELC together

In order to examine the mechanisms of cell-type selectivity of CXCL13/BCA-1 and CCL19/ELC together to rescue cells from TNF-α-mediated apoptosis, we first examined the expression levels of some important substrates of apoptosis pathways in the distinct types of cells at presence of different stimuli during induction of apoptosis. Western blot showed that the protein levels of one group of antiapoptotic members Bcl-2, Bcl-X, and c-FLIP_L in freshly isolated different types of CD19+CD34+ B cells were identical (Figure 6A) (B-CLL B cell data not shown). Interestingly, after stimulation with CXCL13/BCA-1 or/and CCL19/ELC and apoptotic induction with TNF-α, their expression levels were still not significantly changed in different types of CD19+CD34+ B cells (Figure 6A) (CB and B-CLL B cell data not shown). The expression levels of another group of antiapoptotic member proteins in IAP family (XIAP, c-IAP1, c-IAP2, survivin, and livin) in freshly isolated different types of CD19+CD34+ B cells were identical (Figure 6B) (B-CLL B cell data not shown). Interestingly, after stimulation with CXCL13/BCA-1 or/and CCL19/ELC and apoptotic induction with TNF-α, their expression levels were still not significantly changed in different types of CD19+CD34+ B cells (Figure 6B) (CB and B-CLL B cell data not shown).

It was recently reported that stably expression of a novel paternally expressed imprinted gene PEG10 significantly inhibited hepatocellular carcinoma cell apoptotic death (24). To further search the mechanism of CXCL13/BCA-1 and CCL19/ELC together to protect malignant (B-ALL and B-CLL) CD19+CD34+ B cells from TNF-α-mediated apoptosis, we therefore examined the possible roles of PEG10 in CXCL13/CCL19-induced-
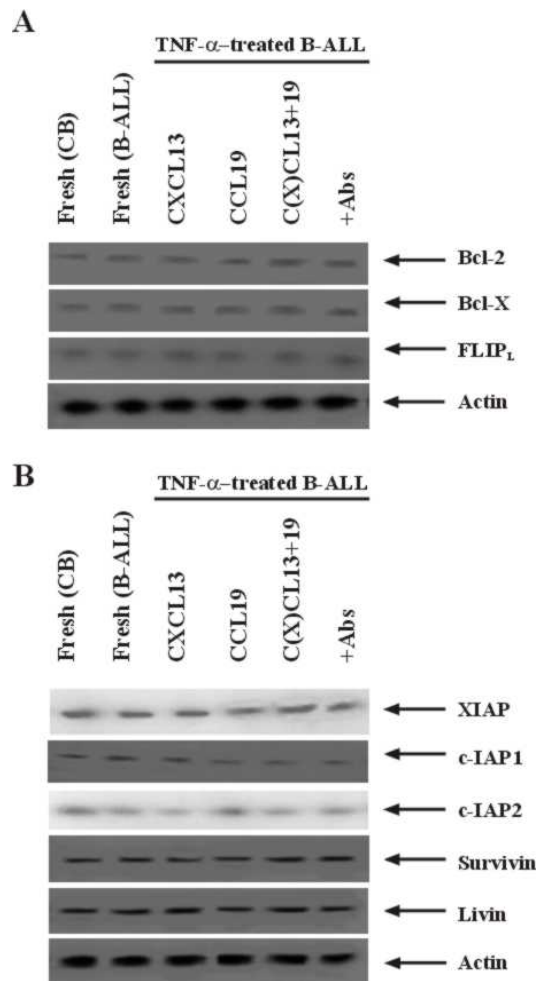

Figure 6. Occurrence of Bcl-2, Bcl-X, c-FLIP_L, and IAP family member protein expression in CD19+CD34+ B cells. The Bcl-2, Bcl-X and c-FLIP_L (A), IAP family member proteins (B) were examined using Western blot analyses. The cells were purified CD19+CD34+ T cells from cord blood (CB) of uncomplicated births and B-ALL patients, which were pre-treated at absence or presence of followed culture in the presence of CXCL13/BCA-1 or/and CCL19/ ELC (all at 100 ng/ml) described in *Materials and Methods*, following stimulation at absence or presence of TNF-α (100 ng/ml) for 24 h at 37° C. They were lysed and total protein content electrophoresed and blotted as described in *Materials and Methods*. Actins indicated the quantity of total cellular protein from the tested samples loaded in each lane. Arrows indicated markers used to verify equivalent molecular weights of appropriate proteins in each lane. The data were from a single experiment, which was representative of six experiments performed.

resistance to TNF-α-mediated apoptosis in B-ALL and B-CLL) CD19+CD34+ B cells. We first examined the expression levels of PEG10 in distinct CD19+CD34+ B cells during the stimulation with CXCL13/CCL19 and TNF-α. Data obtained from real time quantitative RT-PCR and Northern blot analyses (Figure 7) showed that freshly isolated normal peripheral CD19+ T cells and CB CD19+CD34+ B cells expressed almost no PEG10 (Figure 7A) or very low level of PEG10 (Figure 7B). After 24 h culture with CXCL13/BCA-1 or/and CCL19/ELC, levels of PEG10 expression in the cells had not been significantly altered.
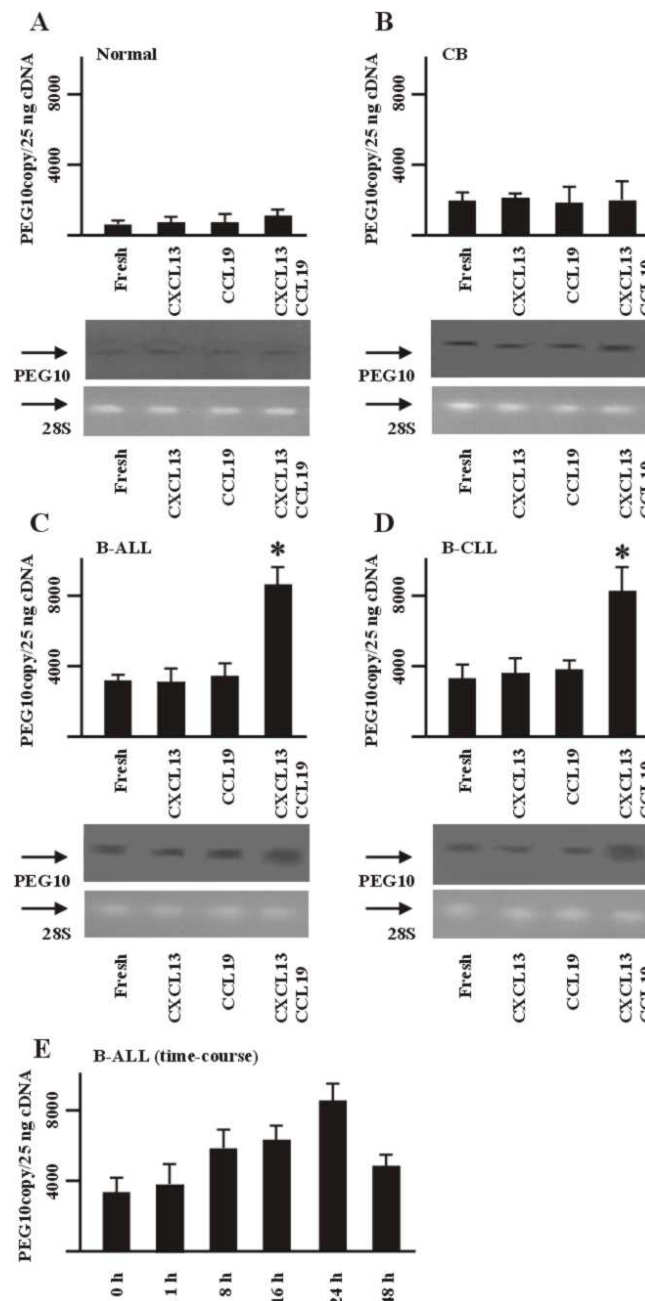
Figure 7. PEG10 mRNA expression in CD19⁺CD34⁺ B cells. The real time quantitative detection of RT-PCR (upper panels) and Northern blot (lower panels) for PEG10 mRNA in the CD19⁺CD34⁺ B cells. The cells were isolated from normal PBMC (only CD19⁺) (A), cord blood (CB) of uncomplicated births (B), B-ALL (C, E) or B-CLL (D) patients as described in *Materials and Methods*, which were pre-treated at absence or presence of chemokine as indicated (all at 100 ng/ml) for 24 h at 37°C, following stimulation with TNF-α (100 ng/ml) for 24 h at 37°C. The procedure for quantitative RT-PCR amplification was described in *Materials and Methods*. A linear relationship between C_T and log starting quantity of standard DNA template or target cDNA (PEG10) was detected (data not shown). The correlation coefficients are approximately 0.97 - 0.99. The showing bars were mean values ± SD of six similar experiments conducted. Total RNA from different cells as indicated were isolated, electrophoresed and blotted as described in *Materials and Methods*. The hybridization signals for PEG10 mRNA in different cells were shown in upper parts of the panels. The 28S rRNAs in lower parts of the panels confirmed the comparable amounts of loaded total RNA. The data were from a single experiment, which was representative of six experiments performed. In E, the real time quantitative detection of RT-PCR for PEG10 mRNA in the CD19⁺CD34⁺ B cells from B-ALL patients as described in *Materials and Methods*, which were pre-treated at absence or presence of CXCL13/BCA-1 and CCL19/ ELC (each 100 ng/ml) for the time intervals as indicated at 37°C.

Co-stimulation with TNF-α did not change the pattern of PEG10 expression levels (data not shown). Interestingly, freshly isolated B-ALL and B-CLL CD19⁺CD34⁺ B cells expressed elevated level of PEG10 (Figure 7C and 7D), compared with that in normal peripheral CD19⁺ T cells and CB CD19⁺CD34⁺ B cells. After 24 h cultures, levels of PEG10 expression in the cells had been significantly up-regulated. The up-regulation was only seen in culture with

Table 2. *Analysis of total dead (necrotic and apoptotic) cells in B-CLL CD19⁺CD34⁺ B cells in different treatments.*

Treatment[a]	CXCL13	CCL19	CXCL13/CCL19[b]
Non-treated	64 ± 15[c]	55 ± 19	15 ± 6
PNA mismatch (2 μM)	65 ± 17	61 ± 19	14 ± 5
DNAPEG10 (2 μM)	61 ± 15	60 ± 18	16 ± 4
PNAPEG10 (0.02 μM)	58 ± 21	67 ± 11	20 ± 10
PNAPEG10 (2 μM)	62 ± 9	66 ± 12	68 ± 14*[d]

a. The purified CD19⁺CD34⁺ B cells from B-ALL patients were cultured for 6 days in the presence or absence of PNAPEG10 antisense at low concentration (0.02 μM) and high concentration (2 μM) as described in *Materials and Methods*.
b. They were then pre-treated at presence of CXCL13/BCA-1 or/and CCL19/ELC (all at 100 ng/ml) described in *Materials and Methods*, following stimulation at presence of TNF-α (100 ng/ml) for 24 h at 37° C.
c. The cells were analyzed by flow cytometry for PI (*y* axis) and FITC-conjugated annexin V (*x* axis) as described in *Materials and Methods*. The data for total dead cells (PI⁻ annexin V⁺ + PI⁺ annexin V⁺) were mean values ± SD of six experiments performed.
d. ∗ indicates *p* < 0.005 (*vs* non-treated).

CXCL13/BCA-1 and CCL19/ELC together, but not with CXCL13/BCA-1 or CCL19/ELC alone (Figure 7C and 7D). Co-stimulation with TNF-α did not change the pattern of PEG10 expression levels (data not shown). The time-course study (Figure 7E) showed that the significant up-regulation of PEG10 mRNA by CXCL13/BCA-1 and CCL19/ELC together was already seen within 8h and reached the peak at 24 h. The data were suggesting that PEG10 expression and activation might involved in the mechanism of resistance to TNF-α-mediated apoptosis in B-ALL and B-CLL CD19⁺CD34⁺ B cells induced by CXCL13/BCA-1 and CCL19/ELC together.

PEG10 expression in B-ALL and B-CLL CD19⁺CD34⁺ B cells was essentially important for resistance to apoptosis increased by CXCL13/BCA-1 and CCL19/ELC together

In order to further analyze the role of PEG10 expression in cell programmed death and mechanism of protective effect of CXCL13/BCA-1 and CCL19/ELC together in TNF-α-mediated apoptosis in B-ALL and B-CLL CD19⁺CD34⁺ B cells, we applied peptide nucleic acid antisense of PEG10 (PNAPEG10) to block the PEG10 expression (37) before assay of CXCL13/CCL19-induced resistance to TNF-α-mediated apoptosis. The results from Northern assays showed that culture with PNAPEG10 at high concentration (2 μM) completely abolished expression of PEG10 in B-ALL and B-CLL CD19⁺CD34⁺ B cells at mRNA levels, whereas, neither low concentration PNAPEG10 (0.02 μM) nor DNAPEG10 nor randomly synthesized PNA mismatch had no such effects (data not shown). The data listed in Table 2 demonstrated that PNAPEG10 at high concentration significantly blocked the effects of CXCL13/BCA-1 and CCL19/ELC together on induction of resistance to TNF-α-mediated apoptosis in B-ALL CD19⁺CD34⁺ B cells, none of low concentration PNAPEG10, DNAPEG10 and randomly synthesized PNA mismatch had such function. All treatments did not alter the patterns of functions of
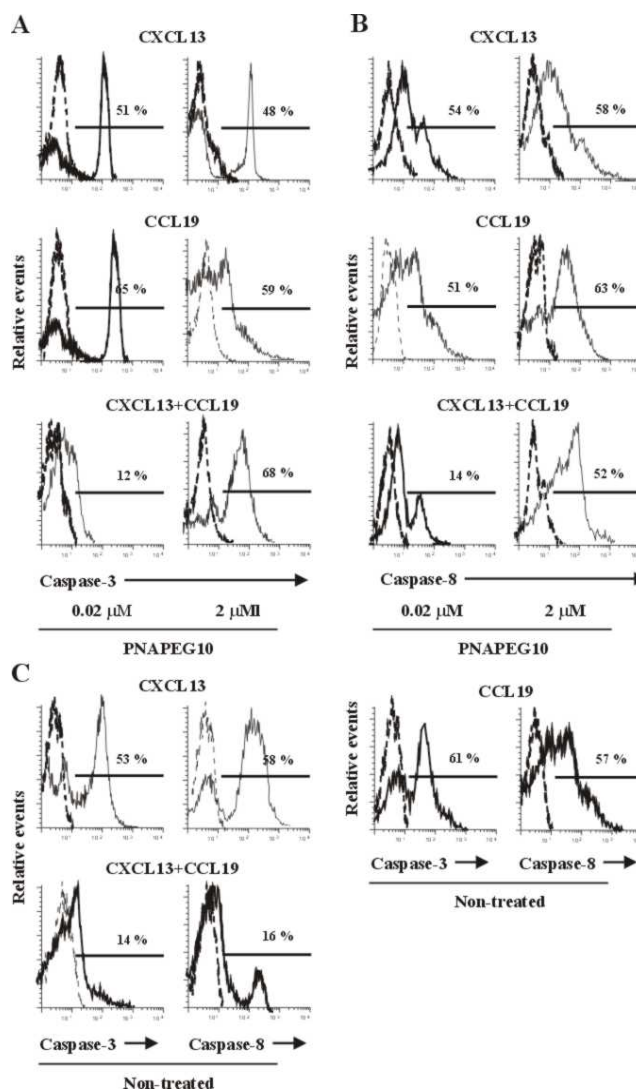

Figure 8. Activation of caspases in CD19⁺CD34⁺ B cells. Flow cytometric analysis of active caspase-3 and caspase-8 in CD19⁺CD34⁺ B cells. The purified CD19⁺CD34⁺ B cells from B-ALL patients were cultured for 6 days in the presence (A and B) or absence (C) of PNAPEG10 antisense at low concentration (0.02 μM) and high concentration (2 μM) as described in *Materials and Methods*. They were then pre-treated at presence of CXCL13/BCA-1 or/and CCL19/ELC (all at 100 ng/ml) described in *Materials and Methods*, following stimulation at presence of TNF-α (100 ng/ml) for 24 h at 37°C. They were then permeabilized and fixed as indicated in *Materials and methods* and subsequently stained for intracellular activated (cleaved) caspase-3 or caspase-8. Activated caspase-3- or caspase-8-specific fluorescence intensity was measured by flow cytometry. The indicating percentages of cells with activated caspase-3 or caspase-8 were quantitated from relative-frequency histograms. Isotype Ab controls were expressed as dished curves.

CXCL13/BCA-1 or CCL19/ELC alone in resistance to TNF-α-mediated apoptosis in B-ALL CD19⁺CD34⁺ B cells (Table 2). The similar results were obtained in B-CLL CD19⁺CD34⁺ B cells (data not shown).

The caspase-3 and caspase-8 expression was essential for programmed cell death (44). Expression levels of activated caspase-3 (Figure 8A) and caspase-8 (Figure 8B)

were measured by intracellular staining of in B-ALL CD19^{+}CD34^{+} B cells in cultures with the distinct treatments. PNAPEG10 at high concentration also significantly blocked the effects of CXCL13/BCA-1 and CCL19/ELC together on stabilization of caspase-3 and caspase-8 in B-ALL CD19^{+}CD34^{+} B cells, meanwhile, none of low concentration PNAPEG10, DNAPEG10 and randomly synthesized PNA mismatch had such function (data not shown). All treatments did not alter the patterns of functions of CXCL13/BCA-1 or CCL19/ELC alone in on stabilization of caspase-3 and caspase-8 in B-ALL CD19^{+}CD34^{+} B cells (Figure 8A and B). As a control, we also measured caspase-3 and caspase-8 expression in un-treated B-ALL CD19^{+}CD34^{+} B cells during TNF-α-mediated apoptosis. The data in Figure 8C showed that PNAPEG10 treatment itself did not change the patterns of caspase-3 and caspase-8 expression during TNF-α-mediated apoptosis, compared with the data in Figure 8A and B. We observed similar results of PNAPEG10 to block stabilization of caspase-3 and caspase-8 expression by CXCL13/BCA-1 and CCL19/ELC together during TNF-α-mediated apoptosis in B-CLL CD19^{+}CD34^{+} B cells (data not shown). Thus, the observation was suggesting that CXCL13/BCA-1 and CCL19/ELC together by means of activation of frequent expressed CXCR5 and CCR7 up-regulated PEG10 expression and function, subsequent stabilized caspase-3 and caspase-8 in B-ALL and B-CLL CD19^{+}CD34^{+} B cells, and rescued the cells from TNF-α-mediated apoptosis. In this event, both CXCR5 and CCR7 signaling together, and PEG10 signaling were necessary.

Since we detected that elevated expression and activation of PEG10 expression during CXCR5-CXCL13/BCA-1- and CCR7-CCL19/ELC-induced resistance to TNF-α-mediated apoptosis in B-ALL and B-CLL CD19^{+}CD34^{+} B cells, we were promoted to further investigate the interactions between mentioned chemokines and their receptors and PEG10 during the events in cells. MCF7 cells were co-transfected with vectors encoding CXCR5 and CCR7 (400 ng each) in the absence or presence of increasing concentrations of PEG10 (100, 400 or 800 ng) as indicated in Figure 9. The data showing in Figure 9A demonstrated that successful transfection of PEG10, CXCR5 and CCR7 took place, documented by Western blot. Flow cytometric analysis (Figure 9B) revealed that only the cells transfected high doses of PEG10 (400 or 800 ng) could be rescued by CXCL13/BCA-1 and CCL19/ELC together from TNF-α-induced apoptosis (Figure 9Bd, e), otherwise, the cells transfected either low dose of PEG10 (100 ng), vector only, or untransfected could not be rescued (Figure 9Ba, b, and c). The transfection itself did not cause apoptosis (Figure 9Bf). Expression levels of activated caspase-3 were measured by intracellular staining in transfected cells. Only in the cells transfected high doses of PEG10 (400 or 800 ng) caspase-3 could be stabilized by CXCL13/BCA-1 and CCL19/ELC together during TNF-α-induced apoptosis (Figure 9Cd, e), otherwise, in the cells transfected either low dose of PEG10 (100 ng), vector only, or untransfected cells caspase-3 could not be stabilized (Figure 9Ca, b, and c). The transfection itself did not cause destabilization (Figure 9Cf). We also obtained the similar results of caspase-8 in the transfected cells (data not
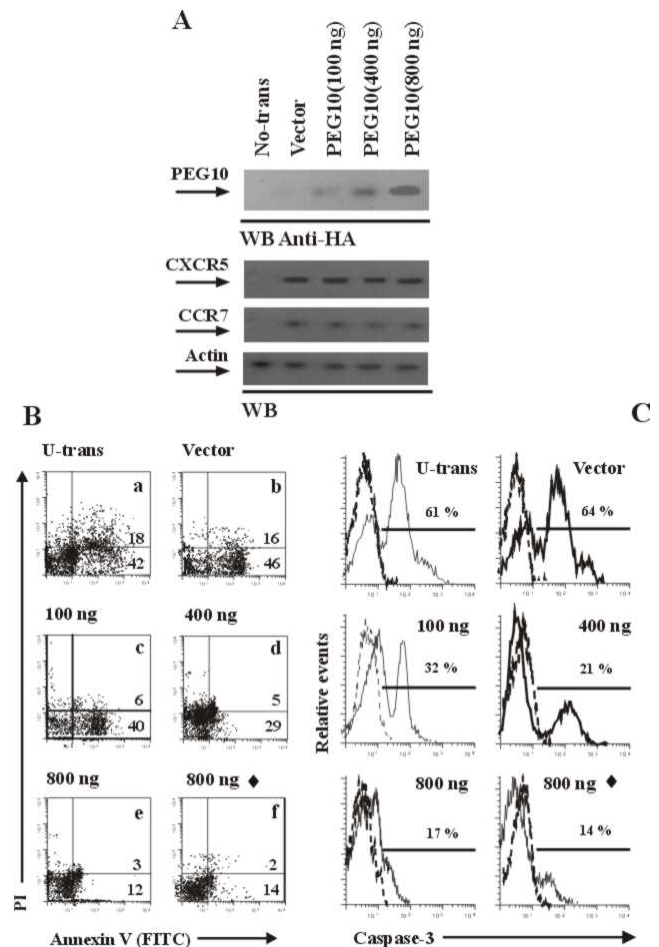

Figure 9. CXCL13/BCA-1 and CCL19/ELC require PEG10 for protection against apoptosis. MCF7 cells were co-transfected with vectors encoding CXCR5 and CCR7 (400 ng each) in the absence or presence of increasing concentrations of PEG10 (100, 400 or 800 ng). The amount of transfected cDNA was kept constant in each sample by adding control pcDNA3 vector. In A, the transfected cells were lysed without stimulation of CXCL13/BCA-1 and CCL19/ELC described in *Materials and Methods*. Western blotting were showing equal expression levels of CXCR5 and CCR7 as well as increasing expression levels of PEG10. In B and C, transfected cells were pre-treated at absence or presence of CXCL13/BCA-1 and CCL19/ELC (all 100 ng/ml) described in *Materials and Methods*, some of cells were followed stimulation with TNF-α (100 ng/ml) for 24 h at 37°C before other assay as indicated ($\blacklozenge$, no stimulation with TNF-α). (B), analysis of total dead (necrotic and apoptotic) cells. The cells were analyzed by flow cytometry as described in the legend for Figure 4. The data were from a single experiment, which was representative of six experiments performed. (C), Flow cytometric analysis of active caspase-3 in transfected cells as indicated. Cells were pre-treated as mentioned above. They were then permeabilized and fixed as indicated in *Materials and methods* and subsequently stained for intracellular activated (cleaved) caspase-3. Activated caspase-3 -specific fluorescence intensity was measured by flow cytometry. The indicating percentages of cells with activated caspase-3 were quantitated from relative-frequency histograms. Isotype Ab controls were expressed as dished curves. The data were from a single experiment, which was representative of six experiments performed.

shown). The results mentioned above were strongly suggesting the necessity of PEG10 in CXCL13/BCA-1 and CCL19/ELC together rescuing cells from TNF-α-mediated apoptosis.

Thus, CXCR5 and CCR7 were selectively frequent expressed on B-ALL and B-CLL CD19$^+$CD34$^+$ B cells. CXCL13/BCA-1 and CCL19/ELC together rescued B-ALL and B-CLL CD19$^+$CD34$^+$ B cells from TNF-α-mediated apoptosis, but not CB CD19$^+$CD34$^+$ B cells. PEG10 expression in B-ALL and B-CLL CD19$^+$CD34$^+$ B cells was selectively increased by CXCL13/BCA-1 and CCL19/ELC together. CXCR5/CXCL13 and CCR7/CCL19 pairs by means of activation of PEG10 increased resistance to apoptosis in B-ALL and B-CLL CD19$^+$CD34$^+$ B cells.

Discussion

The function of homeostatic chemokine receptors and their ligands extends far beyond the induction of transmigration. CXCR5 and CCR7 are recognized as crucial factors in lymphoid system homeostasis and adaptive immunity (1). Both receptors cooperate and contribute to the formation of organizing centers in lymph node and Peyer's patch development. The close cooperation of CXCR5 and CCR7 on cells simultaneously expressing these receptors appears to be a recurrent motif that has been described particularly well for B cell entry, migration and positioning in the spleen (15). B cell arrest in Peyer's patches occurs mainly in follicular HEVs. B cell recruitment into Peyer's patches is mediated by CXCR5 along with CCR7 and CXCR4 (1). Adoptively transferred B cells from CXCR5$^{-/-}$ mice are hampered in homing to Peyer's patches of wildtype mice, and they specifically fail to accumulate in vessels within B cell follicles (10), CXCR5 and CCR7 appear to control B cell positioning during their migration through secondary lymphoid organs. It has long been assumed that B cells first enter T-cell-rich zones of secondary lymphoid organs before they proceed into B-cell follicles (10). However, in Peyer's patches B cells may directly enter follicles via follicular HEVs (10). In contrast, B cells enter the spleen via the marginal zone before they continue to migrate along the outer PALS into the B cell follicles (11). Antigen-engaged B cells are allowed to re-localize to the borders of B cell follicles by differentially regulating their responsiveness towards ligands for CXCR5 and CCR7 (11). Interestingly, not only B cells but also antigen-specific T cells move to the edges of B cell follicles following immunization (45). The interaction of B cells and CD4$^+$ T cells at the edges of B cell follicles eventually leads to B cell proliferation and germinal center formation.

Recent studies have shown that neoplastic cells of hematopoietic and nonhematopoietic origin express various chemokine receptors, and overexpression of some of these has been related to tumor progression and metastasis (46-48). As for B-cell derived lymphoproliferative disorders, CXCR5 have been detected in neoplastic B cells from B-ALL (49) and B-CLL (50). CCR7 has been detected in B-CLL (21) and in tumor cells from classical Hodgkin's disease with lymphocyte predominance (51). In terms of functional *in vitro* activity, only a few studies have addressed chemokine-driven locomotion of neoplastic B

cells. CXCL12 has been shown to enhance chemotaxis of B-ALL and B-CLL (49, 50). The CCR7 ligands, CCL19 and CCL21, enhanced the chemotaxis of B-CLL and Hodgkin's disease cells to CCL19 and CCL21 (21). In the present study, we have investigated four different types of cells, e.g., CD19$^+$CD34$^+$ and CD19$^+$CD34$^-$ B cells from normal CB, B-ALL and B-CLL patients in terms of expression and functions of CXCR5 and CCR7. We have found that CXCR5 and CCR7 are selectively frequent and functionally expressed on B-ALL and B-CLL CD19$^+$CD34$^+$ B cells, meanwhile, B-ALL and B-CLL CD19$^+$CD34$^-$ B cells are expressing them at low level. One novel function of CXCL13/BCA-1 and CCL19/ELC together (but not alone) is that they induce resistance to TNF-α-mediated apoptosis in B-ALL and B-CLL CD19$^+$CD34$^+$ B cells, instead of induction of impressive chemotactic responsiveness.

A majority of the G protein coupled receptor supergene family has been shown to be capable of activating MAPK, which is an indication of providing proliferative or antiapoptotic signaling. It has been reported that several chemokines are able to activate MAPK to function as proliferative or antiapoptotic signals (52). Such as, CXCL12/SDF-1 is an important cytokine acting together with thrombopoietin to enhance the development of megakaryocytic progenitor cells and activates circulating CD34$^+$ cells and platelets (53, 54). CXCL1 and CXCL4 are able to support the survival of endothelial cells and monocytes, respectively (55, 56). Chemokine receptor signaling may be able to provide antiapoptotic activity to hematopoietic cells in a natural context (57). CCR9/CCL25 interaction provides a cell survival signal to the receptor expressing cells (31). However, there are some controversial even contradictory reports. Such as, CXCR4 induces programmed cell death of human peripheral CD4$^+$ T cells, malignant T cells, and CD4/CXCR4 transfectants (58). The interaction between HIV R5 Env and CCR5 activates the Fas pathway and caspase-8 as well as triggering FasL production, ultimately causing CD4$^+$ T cell death (59). We have also reported that CCR3 expression induced by IL-2 and IL-4 functions as a death receptor for B cells (32). The results in this study, together with other observations, suggest that normal B and T cells utilize CXCR5/CXCL13 and CCR7/CCL19 for migration, homing, development, maturation, selection, and cell homeostasis as well as secondary lymphoid tissues organogenesis. Meanwhile, some malignant cells, particularly B-ALL and B-CLL CD19$^+$CD34$^+$ B cells, take advantages of CXCR5/CXCL13 and CCR7/CCL19 for infiltration, resistance to apoptosis, and inappropriate proliferation. To our knowledge, this study is the first report on differential functions of CXCR5/CXCL13 and CCR7/CCL19 in distinct types of cells in terms of induction of apoptotic resistance, and is the direct evidence of the pathophysiological activity of B-ALL and B-CLL CD19$^+$CD34$^+$ B cells induced by CXCL13/BCA-1 and CCL19/ELC together.

PEG10 is identified on human chromosome 7q21 (22, 60). Mouse homologue PEG10 has recently been located in a large imprinted gene cluster on mouse proximal chromosome 6 and has been confirmed to be imprinted (61). Since the protein products from the predicted open reading frames (ORF1 and ORF2) of PEG10 show homology to the gag and pol proteins of vertebrate

retrotransposon Ty3/Gypsy, PEG10 is speculated to be a retrotransposon-derived gene. PEG10 is not completely repressed in adult human tissues. Distinct expression of PEG10 is found in the brain, kidney, lung, testis and placenta but not in the liver and a number of other tissues (22). In contrast to this, expression of PEG10 is only detected in the placenta among the 14 adult mouse tissues examined (61). The PEG10 protein appears to be a cytosolic protein primarily, but a tight association with the nuclear membrane of the cells in interphase was also observed (25). The exact biochemical and biological properties of PEG10 are not yet clear. However, some experimental data suggest a role for preferential expression of the imprinted genes in regulating growth control of liver cells (25). Exogenous expression of PEG10 promotes growth of certain HCC cell lines that does not manifest endogenous expression of this gene. The interaction of PEG10 protein with SIAH proteins plays important roles in resistance to apoptosis (24). Even PEG10 is suggested to serve as a novel molecular target for treatment of HCCs (24). In the present study, we have found that freshly isolated B-ALL and B-CLL CD19$^+$CD34$^+$ B cells expresses elevated level of PEG10, compared with that in normal peripheral CD19$^+$ T cells and CB CD19$^+$CD34$^+$ B cells. After 24h culture with CXCL13/BCA-1 and CCL19/ELC together, levels of PEG10 expression in the cells had been significantly up-regulated (Figure 7). By using PNA antisense assay, we have fond that sufficient PNAPEG10 administration significantly blocks the effects of CXCL13/BCA-1 and CCL19/ELC together on induction of resistance to TNF-α -mediated apoptosis in B-ALL and B-CLL CD19$^+$CD34$^+$ B cells (Table 2). We suggest that CXCL13/BCA-1 and CCL19/ELC together by means of activation of frequent expressed CXCR5 and CCR7 up-regulates PEG10 expression and function, subsequent stabilizes caspase-3 and caspase-8 in B-ALL and B-CLL CD19$^+$CD34$^+$ B cells, and rescues the cells from TNF-α-mediated apoptosis (Figure8 and 9). This is the first time that this imprinted gene has been found to express in both human B-ALL and B-CLL CD19$^+$CD34$^+$ B cells. We also have first time observed that the over-expression of CXCR5 and CCR7 on B-ALL and B-CLL CD19$^+$CD34$^+$ B cells by means of activation of PEG10 mediates resistance to apoptosis in these malignant cells. Understanding the molecular basis of abnormal imprinting of PEG10 in both human B-ALL and B-CLL will shed new light on the process and mechanism that leads to malignant lymphoproliferative disorders.

Acknowledgements

References

1. Muller G, Hopken UE, Lipp M. The impact of CCR7 and CXCR5 on lymphoid organ development and systemic immunity. Immunol Rev. 2003;195:117-135.

2. Sallusto F, Mackay CR, Lanzavecchia A. The role of chemokine receptors in primary, effector, and memory immune responses. Annu Rev Immunol. 2000;18:593-620.

3. Wu MT, Hwang ST. CXCR5-transduced bone marrow-derived dendritic cells traffic to B cell zones of lymph nodes and modify antigen-specific immune responses. J Immunol. 2002;168:5096-5102.

4. Förster R, Emrich T, Kremmer E, Lipp M. Expression of the G-protein-coupled receptor BLR1 defines mature, re-circulating B cells and a subset of T-helper memory cells. Blood. 1994;84:830-840.

5. Saeki H, Wu MT, Olasz E, Hwang ST. A migratory population of skin-derived dendritic cells expresses CXCR5, responds to B lymphocyte chemoattractant *in vitro*, and co-localizes to B cell zones in lymph nodes *in vivo*. Eur J Immunol. 2000;30: 2808-2814.

6. Yu P, Wang Y, Chin RK, et al. B cells control the migration of a subset of dendritic cells into B cell follicles via CXC chemokine ligand 13 in a lymphotoxin-dependent fashion. J Immunol. 2002;168:5117-5123.

7. Ansel KM, Ngo VN, Hyman PL, et al. A chemokine-driven positive feedback loop organizes lymphoid follicles. Nature. 2000;406:309-314.

8. Gunn MD, Ngo VN, Ansel KM, Ekland EH, Cyster JG, Williams LT. A B-cell-homing chemokine made in lymphoid follicles activates Burkitt's lymphoma receptor-1. Nature. 1998;391:799-803.

9. Förster R, Mattis AE, Kremmer E, Wolf E, Brem G, Lipp M. A putative chemokine receptor, BLR1, directs B cell migration to defined lymphoid organs and specific anatomic compartments of the spleen. Cell. 1996;87:1037-1047.

10. Okada T, Ngo VN, Ekland EH, et al. Chemokine requirements for B cell entry to lymph nodes and Peyer's patches. J Exp Med. 2002;196:65-75.

11. Reif K, Ekland EH, Ohl L, et al. Balanced responsiveness to chemoattractants from adjacent zones determines B-cell position. Nature. 2002;416:94-99.

12. Sallusto F, Lenig D, Förster R, Lipp M, Lanzavecchia A. Two subsets of memory T lymphocytes with distinct homing potentials and effector functions. Nature. 1999; 401: 708-712.

13. Yanagihara S, Komura E, Nagafune J, Watarai H, Yamaguchi Y. EBI1/CCR7 is a new member of dendritic cell chemokine receptor that is up-regulated upon maturation. J Immunol. 1998;161:3096-3102.

14. Gunn MD, Tangemann K, Tam C, Cyster JG, Rosen SD, Williams LT. A chemokine expressed in lymphoid high endothelial venules promotes the adhesion and chemotaxis of naive T lymphocytes. Proc Natl Acad Sci USA. 1998;95:258-263.

15. Ohl L, Henning G, Krautwald S, et al. Cooperating mechanisms of CXCR5 and CCR7 in development and organization of secondary lymphoid organs. J Exp Med. 2003; 197:199-204.

16. Luther SA, Lopez T, Bai W, Hanahan D, Cyster JG. BLC expression in pancreatic islets causes B cell recruitment and lymphotoxin-dependent lymphoid neogenesis. Immunity. 2000;12:471-481.

17. Finke D, Acha-Orbea H, Mattis A, Lipp M, Kraehenbuhl J. CD4+CD3- cells induce Peyer's patch development: role of alpha4beta1 integrin activation by CXCR5. Immunity. 2002; 17:363-373.

18. Smith JR, Braziel RM, Paoletti S, Lipp M, Uguccioni M, Rosenbaum JT. Expression of B-cell-attracting chemokine 1 (CXCL13) by malignant lymphocytes and vascular endothelium in primary central nervous system lymphoma. Blood. 2003;101:815-821.

19. Mazzucchelli L, Blaser A, Kappeler A, et al. BCA-1 is highly expressed in Helicobacter pylori-induced mucosa-associated lymphoid tissue and gastric lymphoma. J Clin Invest. 1999; 104:R49-54.

20. Hasegawa H, Nomura T, Kohno M, et al. Increased chemokine receptor CCR7/EBI1 expression enhances the infiltration of lymphoid organs by adult T-cell leukemia cells. Blood. 2000;95:30-38.

21. Till KJ, Lin K, Zuzel M, Cawley JC. The chemokine receptor CCR7 and alpha4 integrin are important for migration of chronic lymphocytic leukemia cells into lymph nodes. Blood. 2002;99:2977-2984.

22. Ono R, Kobayashi S, Wagatsuma H, et al. A retrotransposon-derived gene, peg10, is a novel imprinted gene located on human chromosome 7q21. Genomics. 2001;73:232-237.

23. Okita C, Meguro M, Hoshiya H, Haruta M, Sakamoto YK, Oshimura M. A new imprinted cluster on the human chromosome 7q21-q31, identified by human-mouse mono-chromosomal hybrids. Genomics. 2003;81:556-559.

24. Okabe H, Satoh S, Furukawa Y, et al. Involvement of PEG10 in human hepatocellular carcinogenesis through interaction with SIAH1. Cancer Res. 2003;63:3043-3048.

25. Tsou AP, Chuang YC, Su JY, et al. Overexpression of a novel imprinted gene, PEG10, in human hepatocellular carcinoma and in regenerating mouse livers. J Biomed Sci. 2003;10:625-635.

26. Bennett JM, Catovsky D, Daniel MT, et al. The French-American-British (FAB) Cooperative Group. The morphological classification of acute lymphoblastic leukaemia: concordance among observers and clinical correlation. Br J Haematol. 1981;47:553-558.

27. Cheson BD, Bennett JM, Grever M, et al. National Cancer Institute-sponsored Working Group guidelines for chronic lymphocytic leukemia: revised guidelines for diagnosis and treatment. Blood. 1996;87:4990-4997.

28. Bennett JM, Catovsky D, Daniel MT, et al. Proposals for the classification of chronic (mature) B and T lymphoid leukemias. J Clin Pathol. 1989;42:567-584.

29. Qiuping Z, Qun L, Chunsong H, et al. Selectively increased expression and functions of chemokine receptor CCR9 on CD4$^+$ T cells from patients with T-cell lineage acute lymphocytic leukemia. Cancer Res. 2003;63:6469-6477.

30. Jinquan T, Quan S, Jacobi HH, et al. CXC chemokine receptor 3 expression on CD34(+) hematopoietic progenitors from human cord blood induced by granulocyte-macrophage colony-stimulating factor: chemotaxis and adhesion induced by its ligands, interferon gamma-inducible protein 10 and monokine induced by interferon gamma. Blood. 2000;96:1230-1238.

31. Youn BS, Kim YJ, Mantel C, Yu KY, Broxmeyer HE. Blocking of c-FLIP(L)--independent cycloheximide-induced apoptosis or Fas-mediated apoptosis by the CC chemokine receptor 9/TECK interaction. Blood. 2001;98:925-933.

32. Jinquan T, Jacobi HH, Jing C, et al. CCR3 expression induced by IL-2 and IL-4 functioning as a death receptor for B cells. J Immunol. 2003;171:1722-1731.

33. Kruse N, Pette M, Toyka K, Rieckmann P. Quantification of cytokine mRNA expression by RT PCR in samples of previously frozen blood. J Immunol Methods. 1997;210:195-203.

34. Sica A, Saccani A, Borsatti A, et al. Bacterial lipopoly-saccharide rapidly inhibits expression of C-C chemokine receptors in human monocytes. J Exp Med. 1997;185:969-974.

35. Massari P, Ho Y, Wetzler LM. Neisseria meningitidis porin PorB interacts with mitochondria and protects cells from apoptosis. Proc Natl Acad Sci U S A. 2000;97:9070-9075.

36. Nguyen DH, Taub D. CXCR4 function requires membrane cholesterol: implications for HIV infection. J Immunol. 2002;168:4121-4126.

37. Norton JC, Piatyszek MA, Wright WE, Shay JW, Corey DR. Inhibition of human telomerase activity by peptide nucleic acids. Nat Biotechnol. 1996;14:615-619.

38. Kanbe K, Shimizu N, Soda Y, Takagishi K, Hoshino H. A CXC chemokine receptor, CXCR5/BLR1, is a novel and specific coreceptor for human immunodeficiency virus type 2. Virology. 1999;265:264-273.

39. Campbell JJ, Qin S, Bacon KB, Mackay CR, Butcher EC. The biology of chemokine and classical chemoattractant receptors: differential requirements for adhesion-triggering versus chemotactic responses in lymphoid cells. J Cell Biol. 1996;134:255-266.

40. Youn BS, Mantel C, Broxmeyer HE. Chemokines, chemokine receptors and hematopoiesis. Immunol Rev. 2000;177:150-174.

41. Kampen GT, Stafford S, Adachi T, et al. Eotaxin induces degranulation and chemotaxis of eosinophils through the activation of ERK2 and p38 mitogen-activated protein kinases. Blood. 2000;15:1911-1917.

42. Boehme SA, Sullivan SK, Crowe PD, et al. Activation of mitogen-activated protein kinase regulates eotaxin-induced eosinophil migration. J Immunol. 1999;163:1611-1618.

43. Wang JF, Park IW, Groopman JE. Stromal cell-derived factor-1alpha stimulates tyrosine phosphorylation of multiple focal adhesion proteins and induces migration of hematopoietic progenitor cells: roles of phosphoinositide-3 kinase and protein kinase C. Blood. 2000;95:2505-2513.

44. Thornberry NA, Lazebnik Y. Caspases: enemies within. Science. 1998;281:1312-1316.

45. Garside P, Ingulli E, Merica RR, Johnson JG, Noelle RJ, Jenkins MK. Visualization of specific B and T lymphocyte interactions in the lymph node. Science. 1998;281:96-99.

46. Muller A, Homey B, Soto H, et al. Involvement of chemokine receptors in breast cancer metastasis. Nature. 2001;410:50-56.

47. Geminder H, Sagi-Assif O, Goldberg L, et al. A possible role for CXCR4 and its ligand, the CXC chemokine stromal cell-derived factor-1, in the development of bone marrow metastases in neuroblastoma. J Immunol. 2001;167:4747-4757.

48. Scotton CJ, Wilson JL, Milliken D, Stamp G, Balkwill FR. Epithelial cancer cell migration: a role for chemokine receptors? Cancer Res. 2001;61:4961-4965.

49. Durig J, Schmucker U, Duhrsen U. Differential expression of chemokine receptors in B cell malignancies. Leukemia. 2001;15:752-756.

50. Burger JA, Burger M, Kipps TJ. Chronic lymphocytic leukemia B cells express functional CXCR4 chemokine receptors that mediate spontaneous migration beneath bone marrow stromal cells. Blood. 1999;94:3658-3667.

51. Hopken UE, Foss HD, Meyer D, et al. Up-regulation of the chemokine receptor CCR7 in classical but not in lymphocyte-predominant Hodgkin disease correlates with distinct dissemination of neoplastic cells in lymphoid organs. Blood. 2002;99:1109-1116.

52. Ganju RK, Brubaker SA, Meyer J, et al. The α-chemokine, stromal cell-derived factor-1alpha, binds to the transmembrane G-protein-coupled CXCR-4 receptor and activates multiple signal transduction pathways. J Biol Chem. 1998;273:23169-23175.

53. Hodohara K, Fujii N, Yamamoto N, Kaushansky K. Stromal cell-derived factor-1 (SDF-1) acts together with thrombopoitin to enhance the development of megakaryocytic progenitor cells (CFU-MK). Blood. 2000;95:769-775.

54. Lataillade JJ, Clay D, Dupuy C, et al. Chemokine SDF-1 enhances circulat-ing CD34+ cell proliferation in synergy with cytokines: Possible role in progenitor survival. Blood. 2000;95:756-768.

55. Han ZC, Lu M, Li J, et al. Platelet factor 4 and other CXC chemokines support the survival of normal hematopoietic

cells and reduce the chemosensitivity of cells to cytotoxic agents. Blood. 1997;89:2328-2335.

56. Scheuerer B, Ernst M, Durrbaum-Landmann I, et al. The CXC chemokine platelet factor 4 promotes survival and induce monocyte differentiation into macrophages. Blood. 2000;95:1158-1166.

57. Youn BS, Yu KY, Oh J, Lee J, Lee TH, Broxmeyer HE. Role of the CC chemokine receptor 9/TECK interaction in apoptosis. Apoptosis. 2002;7:271-276.

58. BerndtC., Mopps B, Angermuller S, Gierschik P, Krammer PH. CXCR4 and CD4 mediate a rapid CD95-independent cell death in CD4$^+$ T cells. Proc Natl Acad Sci U S A. 1998;95:12556-12561.

59. Algeciras-Schimnich A, Vlahakis SR, Villasis-Keever A, et al. CCR5 mediates Fas- and caspase-8 dependent apoptosis of both uninfected and HIV infected primary human CD4 T cells. AIDS. 2002;16:1467-1478.

60. Nakabayashi K, Bentley L, Hitchins MP, et al. Identification and characterization of an imprinted antisense RNA (MESTIT1) in the human MEST locus on chromosome 7q32. Hum Mol Genet. 2002;11:1743-1756.

61. Ono R, Shiura H, Aburatani H, Kohda T, Kaneko-Ishino T, Ishino F. Identification of a large novel imprinted gene cluster on mouse proximal chromosome 6. Genome Res. 2003;13: 1696-1705.